Int. J. Solids Structures Vol. 30, No. 16, pp. 2143–2161, 1993
Printed in Great Britain

0020–7683/93 $6.00+ .00

DELAMINATION CRACKS ORIGINATING FROM TRANSVERSE CRACKING IN CROSS-PLY LAMINATES UNDER VARIOUS LOADINGS

YUJUN KIM and SEYOUNG IM
Department of Mechanical Engineering, Korea Advanced Institute of Science and Technology, Science Town, Taejeon, 305-701, Republic of Korea

(*Received* 8 *November* 1992; *in revised form* 5 *March* 1993)

Abstract—Delamination cracks originating from transverse cracking in two types of cross-ply laminates $[90/0]_s$ and $[0/90]_s$ are analysed for three types of loadings: plane strain extension, plane strain bending and antiplane shear. The asymptotic solution for stress and displacement field is constructed based upon the Stroh formalism for anisotropic elasticity and the method of eigenfunction expansion. Its structure is determined from appropriate near-field conditions leading to the eigenvalue equation, and then the singular hybrid finite element method in conjunction with a quadratic programming procedure for treating the partial contact of crack faces is employed to complete the field solution. The stress intensity factor properly defined for anisotropic interfacial cracks and the energy release rate are computed from the complete solution. The stability of crack growth and the effect of the relative ply thickness upon the crack growth stability are examined in terms of the energy release rate and the phase angle.

1. INTRODUCTION

Fiber reinforced composite laminates, which have increasing applications in engineering structures for many products of small or large scale, generally retain many initial flaws such as voids and fiber breakage, and moreover geometric or material discontinuities such as free edge, ply interface, cutout, or re-entry corner etc. The local stress field near such flaws and discontinuities is severely perturbed, and this intense localized stress field gives rise to initiation and growth of cracks or flaws, which gradually lead to a degradation of strength and stiffness before final failure. Thus the accurate stress analysis for such localized discontinuity or flaw zones in a composite laminate is very important in relation to the understanding of its fundamental fracture or failure behavior, and has received significant attention in the composite material community: among the well-known examples are free edge problems, transverse crack problems and delamination crack problems.

After Pipes and Pagano (1970) first employed the finite difference method to study the interlaminar stress in symmetric composite laminates under extension, the stress singularities and stress distributions near the free edge in anisotropic composite laminates were reported by Zwiers *et al.* (1982) and Wang and Choi (1982). In the same way as the free edge problems, Wang (1984) and Wang and Choi (1983) treated the problems of delamination cracks in anisotropic composite laminates. The stress singularities near the transverse cracks in anisotropic composite laminates were first reported by Ting and Hoang (1984) although the solutions to the similar problems in isotropic bi-materials were somewhat earlier reported by Bogy (1971). Im (1989) calculated the stress singularities and computed the asymptotic stress fields near such transverse cracks in cross-ply laminates. Recently, it was reported that as the load increases, transverse cracks occurring in the 90° ply of cross-ply laminates terminating at the interface tend to kink into delamination cracks along the ply interface (Lim, 1988). Kim *et al.* (1991) treated such delamination cracks in cross-ply laminates under plane strain extension by use of the boundary collocation technique.

The purpose of the present work is to examine the fracture behavior of the cross-ply laminates containing delamination cracks originating from transverse cracking under various loadings, with the aid of singular hybrid finite element method combined with the asymptotic solution near the crack tip. In terms of the energy release rate and the phase angle, the stability of crack growth and the effect of geometric parameters such as crack

length and relative ply thickness are examined under three types of loadings: plane strain extension, bending and antiplane shear.

In Section 2, the problem under consideration is stated, and then based upon the Stroh formalism for anisotropic elasticity, the general solutions for stress and displacement fields in cross-ply laminates are obtained. The asymptotic solutions obtained from the eigenfunction expansion are presented in Section 3. The appropriate near-field conditions are imposed to lead to the eigenvalue equations, which determine the structures of the asymptotic solutions, including the stress singularities. In Section 4, the asymptotic solutions, determined within the unknown constants, are then incorporated into the singular hybrid crack-tip finite elements, which are combined with the regular finite elements to complete the solution. Solution procedure for treating the contact problems is taken to consider possible partial closure of crack faces. It turns out that the crack faces in $[0/90]_s$ under plane strain extension are slightly opened near the crack tip although the remaining greater part of the faces are closed, as opposed to the contention of Kim *et al.* (1991) that the crack faces for $[0/90]_s$ are fully closed under the plane strain extension. In Section 5, the numerical results obtained from the singular hybrid FEM are shown in terms of the stress intensity factor clearly defined by Suo (1990). The crack growth stability versus the crack length is discussed in terms of the energy release rate and the phase angle for each of the plane strain extension, the plane strain bending and the antiplane shear, and the effect of thickness upon the energy release rate trend is discussed.

2. STATEMENT OF THE PROBLEM AND BASIC EQUATIONS

Consider two types of cross-ply composite laminates, $[90/0]_s$ and $[0/90]_s$ under plane strain extension or bending, or antiplane shear deformation. As the load increases, there will occur numerous transverse cracks running parallel to the fiber orientation of the 90° ply, with an approximately uniform spacing along the length of the laminates. These cracks, extending perpendicularly to the ply interface and terminating right there because of the stronger 0° ply, tend to develop into delamination cracks along the interface as the load increases further (Kim *et al.*, 1991). To simplify the problem, we assume that the cracks are uniformly arranged, so that the overall arrangement is obtained by repetition of the representative unit cell (see Fig. 1).

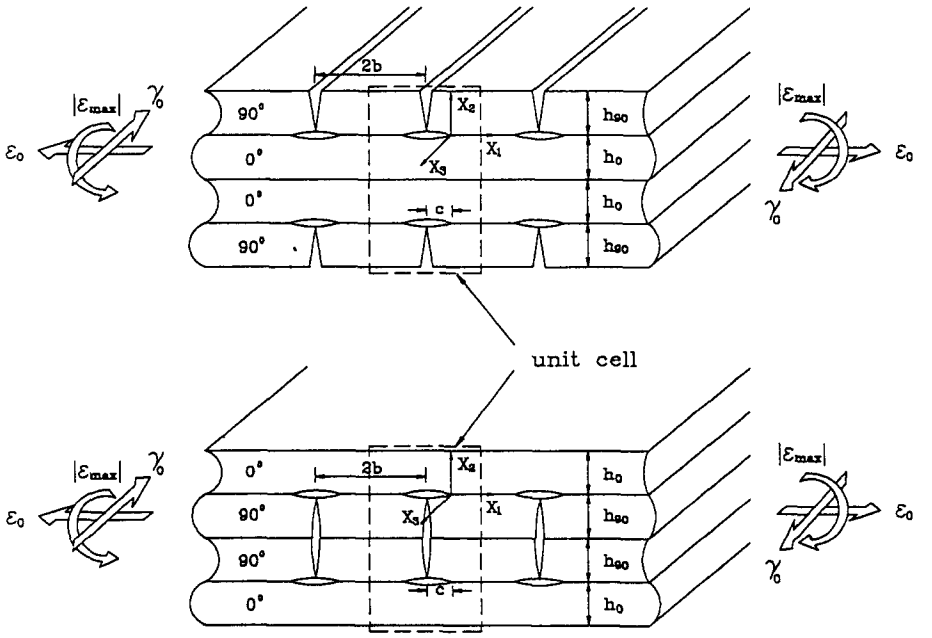

Fig. 1. Delamination cracks originating from transverse cracking in $[90/0]_s$ and $[0/90]_s$.

A rectangular Cartesian coordinate system is taken with its origin at a crack tip; the x_1 axis is along the crack ligament while the x_2 axis is taken to be perpendicular to the interface, and then the x_3 axis lies along the direction which is parallel to the cracks (see Fig. 1). Then each ply of the laminates lies in a plane parallel to the x_1–x_3 plane, and the ply orientation θ is given by the counterclockwise angle, viewed from the top, that the fiber direction makes with the x_1 axis. The laminates have sufficiently large dimension in the x_3 direction, compared with the dimension in the x_2 direction; the laminates are then assumed to be in the state of plane strain deformation under extension or bending, wherein the displacement in the x_3 axis disappears identically, and to be in the state of antiplane deformation under shear, where the displacements in the x_1 and x_2 axes are identically zero. Moreover, the deformation field is a function of only the two coordinates x_1 and x_2.

In a fixed rectangular Cartesian coordinate, let u_i, σ_{ij}, ε_{ij}, C_{ijkl} be the displacement, stress, strain and fourth-order stiffness components, respectively. Then we have the governing equations of equilibrium, strain–displacement relations and stress–strain relations:

$$\sigma_{ij,j} = 0, \tag{1a}$$

$$\varepsilon_{ij} = (u_{i,j}+u_{j,i})/2, \tag{1b}$$

$$\sigma_{ij} = C_{ijkl}\varepsilon_{kl}, \tag{1c}$$

$$C_{ijkl} = C_{jikl} = C_{klij},$$

where summation is implied on the repeated indices, and a comma indicates partial differentiation with respect to x_α ($\alpha = 1, 2$). Hereafter the lower case Roman indices are used to indicate 1, 2 or 3 unless stated otherwise, while the Greek letters indicate 1 or 2.

For the aforementioned types of deformations, we can assume (Ting, 1986) that

$$z = x_1 + px_2,$$

$$u_k = v_k H(z), \tag{2}$$

where p and v_k are, respectively, the eigenvalue and eigenvector to be determined, and H is a function of z. Substitution of eqn (2) into eqn (1a, b, c) yields

$$\sigma_{ij} = \sum_{k=1}^{3} (C_{ijk1}+pC_{ijk2})v_k \, \mathrm{d}H(z)/\mathrm{d}z, \tag{3}$$

$$\sum_{k=1}^{3} \{C_{i1k1}+p(C_{i1k2}+C_{i2k1})+p^2C_{i2k2}\}v_k = 0. \tag{4}$$

For the existence of nontrivial solutions v_k, we have

$$\det[C_{i1k1}+p(C_{i1k2}+C_{i2k1})+p^2C_{i2k2}] = 0. \tag{5}$$

This results in the sextic equation for the eigenvalue p and then the eigenvector v_k is obtained from eqn (4). Because of material symmetry of the orthotropic materials such as $[90/0]_s$ and $[0/90]_s$ laminates (Kim *et al.*, 1991), eqn (5) is decomposed into two, a quadratic and a quartic equation in p. Let ξ_α ($\alpha = 1, 2$) denote a root of the quadratic equation and μ_i ($i = 1, 2, 3, 4$) a root of the quartic equation. The eigenvalues ξ_α are associated with the antiplane shear deformation, which involves only the displacement u_3, and μ_i are related to plane strain deformation involving the displacement u_1 and u_2. Then the ξ_1 and ξ_2 become complex conjugate to each other. Similarly, we can confirm that the μ_i ($i = 1, 2, 3, 4$) constitute two complex conjugate pairs [refer to Kim *et al.* (1991) and references cited therein]. Two deformation modes, the antiplane shear deformation and the plane strain deformation, are decoupled from each other. The associated eigenvectors v_k for each of the

eigenvalues ξ_α and μ_i will be denoted by $v_{k\alpha}$ and v_{ki}. General solutions for two types of deformations are written, respectively, as [see Kim *et al.* (1991) for details]:

antiplane shear deformation:

$$s_\alpha = x_1 + \xi_\alpha x_2,$$

$$u_3 = \sum_{\alpha=1}^{2} v_{3\alpha} F(s_\alpha), \tag{6a}$$

$$\sigma_{3\beta} = \sum_{\alpha=1}^{2} (C_{3\beta 31} + \xi_\alpha C_{3\beta 32}) v_{3\alpha} \frac{\mathrm{d}F(s_\alpha)}{\mathrm{d}s_\alpha}; \tag{6b}$$

plane strain deformation:

$$z_k = x_1 + \mu_k x_2 \quad (k = 1, 2, 3, 4),$$

$$u_\alpha = \sum_{k=1}^{4} v_{\alpha k} G(z_k), \tag{7a}$$

$$\sigma_{\alpha\beta} = \sum_{k=1}^{4} \sum_{\gamma=1}^{2} (C_{\alpha\beta\gamma 1} + \mu_k C_{\alpha\beta\gamma 2}) v_{\gamma k} \frac{\mathrm{d}G(z_k)}{\mathrm{d}z_k}. \tag{7b}$$

Here F and G are functions of s_α and z_k, respectively. It is noted that the foregoing development holds for each ply, and we will use the superscript (1), (2) to denote the upper and lower ply, respectively. Since the case of plane strain extension was treated by Kim *et al.* (1991), our attention is primary given to the case of plane strain bending and antiplane shear, and just some corrective remarks on the previous results (Kim *et al.*, 1991) are to be made for the plane strain extension.

3. ASYMPTOTIC SOLUTIONS FOR STRESS AND DISPLACEMENT NEAR THE CRACK TIP

Historically, an eigenfunction denoting the asymptotic field solution near the crack tip has been used in a form of the power series, as assumed by Williams (1959). Dempsey and Sinclair (1979) showed that in a certain problem of composite wedges fails the application of power-type eigenfunctions, and then they introduced the logarithmic eigenfunction. Ting and Chou (1981) extended this view to the problem of anisotropic composite laminates. For the present problem, however, the power-type eigenfunction (Wang and Choi, 1982; Ting and Hoang, 1984; Ting, 1986) successfully represents the asymptotic solution, that is, the set of eigenvectors sufficient to span its solution exists.

To determine the structure of the asymptotic solution including the stress singularities, we need to consider the near-field conditions that the solution is required to meet near the crack tip. We assume that all crack faces are frictionless, and along the crack ligament the two plies are bonded perfectly to each other. Then for antiplane shear the conditions on the crack faces and on the ligament are summarized as [for plane strain deformation, refer to Kim *et al.* (1991)]

$$\sigma_{23}^{(1)}(x_1, 0^+) = \sigma_{23}^{(2)}(x_1, 0^-) = 0 \quad \text{on the crack faces } (x_1 \leqslant 0), \tag{8a}$$

$$[\sigma_{23}(x_1, 0)] = [u_3(x_1, 0)] = 0 \quad \text{on the ply interfaces } (x_1 \geqslant 0), \tag{8b}$$

where the superscript (1) or (2) indicates the upper or the lower ply, respectively, and the bracket [ ] denote discontinuity of the quantity in it across the ply interface. Note that we do not know *a priori* whether the crack faces are opened or closed for the plane strain deformation. It depends upon the geometry as well as the loading, and therefore we need to obtain the complete solution for this. The problem becomes nonlinear when the contacts of crack faces are involved. To deal with such a contact problem, we will introduce a special technique in the solution procedure later. For the time being, we proceed to obtain the asymptotic solution, implicitly assuming that either opening or closure has been chosen.

For antiplane shear deformation first, we assume the power type eigenfunction as given by Ting (1986)

$$F(s_\alpha) = \sum_{n=1}^{\infty} A_{\alpha n} s_\alpha^{\delta_n+1}/(\delta_n+1),$$

$$s_\alpha = x_1 + \xi_\alpha x_2.$$

Rewriting eqn (6a, b) to denote the displacement and stress field for this deformation, we have

$$u_3^{(m)} = \sum_{n=1}^{\infty}\sum_{\alpha=1}^{2} A_{\alpha n}^{(m)} v_{3\alpha}^{(m)} s_\alpha^{(m)\delta_n+1}/(\delta_n+1) \qquad (m=1,2), \tag{9a}$$

$$\sigma_{3\beta}^{(m)} = \sum_{n=1}^{\infty}\sum_{\alpha=1}^{2} A_{\alpha n}^{(m)} (C_{3\beta 31}^{(m)} + \xi_\alpha^{(m)} C_{3\beta 32}^{(m)}) v_{3\alpha}^{(m)} s_\alpha^{(m)\delta_n} \qquad (m=1,2), \tag{9b}$$

where the superscript $m = 1, 2$ indicates one of the two different plies, respectively. Because these solutions are required to satisfy the near-field conditions, substitution of eqn (9a, b) into eqn (8a, b) yields the 4×4 homogeneous linear algebraic equations

$$\sum_{j=1}^{4} \Delta_{ij}(\delta_n) D_{jn} = 0 \quad (i, j = 1, 2, 3, 4),$$

$$D_{\alpha n} = A_{\alpha n}^{(1)}, \quad D_{(\alpha+2)n} = A_{\alpha n}^{(2)} \quad (\alpha = 1, 2), \tag{10}$$

where "(1)", "(2)" denote the upper and lower ply, respectively. For the existence of nontrivial solutions D_{jn}, we have

$$\det[\Delta_{ij}(\delta_n)] = 0, \tag{11}$$

which determines the eigenvalue δ_n. From the structure of Δ_{ij}, we can show that if δ_n is the root of the characteristic equation (11), so is its complex conjugate $\bar{\delta}_n$, so that the expressions for the stress and displacement may become real. Thus, when $A_{\alpha n}^{(m)}$ and $A_{\alpha \bar{n}}^{(m)}$ indicate the corresponding eigenvectors for δ_n and $\bar{\delta}_n$, respectively, they have the following conjugate relation as

$$A_{1n}^{(m)} = \bar{A}_{2\bar{n}}^{(m)}, \quad A_{2n}^{(m)} = \bar{A}_{1\bar{n}}^{(m)} \quad \text{if } \delta_n \text{ is complex},$$
$$A_{2n}^{(m)} = \bar{A}_{1n}^{(m)} \quad \text{if } \delta_n \text{ is real}. \tag{12a}$$

For convenience, we take

$$A_{\alpha n}^{(m)} = \tfrac{1}{2}(\gamma_{1n} - i\gamma_{2n}) a_{\alpha n}^{(m)} \quad \text{for complex } \delta_n, \ \mathrm{Im}[\delta_n] > 0,$$
$$A_{\alpha n}^{(m)} = \tfrac{1}{2}\gamma_{3n} a_{\alpha n}^{(m)} \quad \text{for real } \delta_n \quad (\text{no sum on } n). \tag{12b}$$

Here $a_{\alpha n}^{(m)}$ is the solution of the eigenvector $A_{\alpha n}^{(m)}$, depending upon the associated eigenvalue δ_n, and within an arbitrary constant it can be computed from eqn (10) when properly normalized. Now γ_{in} $(i = 1, 2, 3)$ are real constants to be determined to complete the asymptotic solution. We can then rewrite the asymptotic stress and displacement solution, eqn (9a, b), as

$$u_3^{(m)} = \sum_{n=1}^{\infty} Q_{n3}^{(m)}, \quad \sigma_{3\alpha}^{(m)} = \sum_{n=1}^{\infty} P_{n3\alpha}^{(m)}, \tag{13a, b}$$

where $Q_{n3}^{(m)}$ and $P_{n3\alpha}^{(m)}$ are given in Appendix A.

For plane strain deformation, we take the power type eigenfunction as

$$G(z_k) = \sum_{n=1}^{\infty} B_{kn} z_k^{\delta_n+1}/(\delta_n+1),$$

$$z_k = x_1 + \mu_k x_2 \quad (k = 1,2,3,4).$$

Then following the same procedure as in the antiplane shear deformation and referring to Kim *et al.* (1991), we obtain the asymptotic solution of displacement and stress field as

$$u_\alpha^{(m)} = \sum_{n=1}^{\infty} Q_{n\alpha}^{(m)}, \quad \sigma_{\alpha\beta}^{(m)} = \sum_{n=1}^{\infty} P_{n\alpha\beta}^{(m)}, \tag{14a, b}$$

where $Q_{n\alpha}^{(m)}$ and $P_{n\alpha\beta}^{(m)}$ are described in Appendix A.

The unknown real constants γ_{in} $(i = 1,2,3)$ should be obtained through the numerical solution procedure such as the boundary collocation method (Wang and Choi, 1982), the singular hybrid finite element method (Wang, and Yuan, 1983), or the enriched finite element method (Atluri and Nakagaki, 1986; Stolarski and Chiang, 1989). We here use the singular hybrid finite element method, devising a singular hybrid element into which the asymptotic solution near the crack tip is embedded. This approach can be combined with Lemke's algorithm (Lemke, 1968) to treat the complementary problem resulting from the contact problem, and it is therefore appropriate particularly for plane strain bending or extension where the crack faces may be in partial contact with each other; moreover the hybrid finite element approach is valid for a wide range of crack sizes compared with the boundary collocation method, which turns out to encounter a difficulty when the crack size is very small compared with the ligament length (see Section 5 for details). The asymptotic solution truncated is written as

$$\sigma_{ij} = \sum_{n=1}^{N} \beta_n f_{ij}^n(x_1, x_2, \delta_n), \tag{15a}$$

$$u_i = \sum_{n=1}^{N} \beta_n g_i^n(x_1, x_2, \delta_n), \tag{15b}$$

where β_n denote the unknown constants γ_{in} for each deformation, say, $\beta_1 = \gamma_{11}$, $\beta_2 = \gamma_{21}$, $\beta_3 = \gamma_{31}, \ldots$ etc., when δ_1 is complex and δ_2 is real, and N is the total number of the eigenvalues truncated, which may be different for each deformation.

4. NUMERICAL SOLUTION PROCEDURE

To obtain the complete solution over the entire domain, we rely upon a special finite element method, where a singular hybrid element, used to model the crack tip, is incorporated with eight node iso-parametric regular elements of its surrounding. The asymptotic solution truncated properly is embedded into the singular hybrid element so that the near-tip field is matched with the far-field solution represented by the surrounding regular elements. Kim *et al.* (1991) treated the case of the plane strain extension by use of the boundary collocation method, assuming that the crack faces are either fully opened or fully closed, which must be confirmed after the complete solution. However in case there occurs partial contact or opening of the crack faces, the boundary collocation method is not straightforwardly applicable, but requires some iteration procedure implemented for dealing with the contact boundary. On the other hand, the present finite element scheme may be easily combined with Lemke's algorithm (Lemke, 1968) to treat the contact problem efficiently. Moreover, the finite element method has an advantage over the boundary collocation method in that the former yields uniformly accurate solution regardless of the size of the delamination crack relative to the length of the crack ligament. As will be discussed in the next section, the boundary collocation method encounters a difficulty of very large boundary residuals for very short crack size; from this the eigenfunction series

is seen to fail to represent the far-field solution when the crack length is very small compared with the laminates dimension.

4.1. *Formulation of the singular hybrid element*

To illustrate the basic scheme of stiffness matrix formulation for the singular elements, we follow the line adopted by Wang and Yuan (1983). We first consider each singular region around a crack tip covered with a single hybrid element into which the asymptotic representation is incorporated. The asymptotic solution in the near-tip field of the hybrid element is matched with the far-field solution represented by the regular finite elements surrounding the hybrid element. It is then needed, in addition to the asymptotic solution, that the displacement $\bar{\mathbf{u}}$ along the boundary between the singular element and the regular elements is assumed independently. The stiffness matrix of singular element is formulated on the basis of the hybrid variational functional $\Pi_{mh}(\boldsymbol{\sigma}, \mathbf{u}, \bar{\mathbf{u}})$ in Washizu (1988), which can be derived from the Reissner–Hellinger variational functional with a relaxed continuity condition along the interelement boundary with the aid of Lagrangian multiplier technique. For the present problem, the asymptotic solution (15a, b) for stress and displacement, which will be embedded into the singular hybrid element, satisfies all governing equations except for the interelement compatibility with the surrounding regular elements, so that the functional Π_{mh} can be written as [see Wang and Yuan (1983) for details]

$$\Pi_{mh} = \int_{\partial A_m} \mathbf{T}^{\mathrm{T}} \bar{\mathbf{u}} \, \mathrm{d}s - \frac{1}{2} \int_{\partial A_m} \mathbf{T}^{\mathrm{T}} \mathbf{u} \, \mathrm{d}s, \tag{16}$$

where A_m is the area of the mth singular hybrid element; ∂A_m is the boundary of A_m, and $\mathbf{T}$ is the traction.

Equation (15a, b) may be written in the matrix forms

$$\boldsymbol{\sigma} = \mathbf{P}\boldsymbol{\beta}, \quad \mathbf{u} = \mathbf{U}\boldsymbol{\beta}, \tag{17a, b}$$

and the matrix notation for $\mathbf{T}$ can be found from the expression (17a):

$$\mathbf{T} = \mathbf{R}\boldsymbol{\beta}. \tag{18}$$

For the displacement along the boundary of a hybrid element, we introduce the standard quadratic interpolation function, $\mathbf{L}$, to ensure proper matching with boundary displacement of the adjacent eight node iso-parametric nonsingular elements as follows:

$$\bar{\mathbf{u}} = \mathbf{L}\mathbf{q}, \tag{19}$$

where $\mathbf{q}$ is the nodal degree of freedom common to the hybrid element and the surrounding regular elements. Now the functional Π_{mh} can be written as

$$\Pi_{mh} = \boldsymbol{\beta}^{\mathrm{T}} \mathbf{G}\mathbf{q} - \tfrac{1}{2}\boldsymbol{\beta}^{\mathrm{T}} \mathbf{H}\boldsymbol{\beta}, \tag{20}$$

where

$$\mathbf{G} = \int_{\partial A_m} \mathbf{R}^{\mathrm{T}} \mathbf{L} \, \mathrm{d}s, \quad \mathbf{H} = \frac{1}{2} \int_{\partial A_m} (\mathbf{R}^{\mathrm{T}} \mathbf{U} + \mathbf{U}^{\mathrm{T}} \mathbf{R}) \, \mathrm{d}s.$$

The stationary property of the first variation of Π_{mh} leads to

$$\boldsymbol{\beta} = \mathbf{H}^{-1} \mathbf{G}\mathbf{q}. \tag{21}$$

Substitution of eqn (21) into (20) yields

$$\Pi_{mh} = \tfrac{1}{2}\mathbf{q}^{\mathrm{T}}\mathbf{k}_s\mathbf{q}, \quad \mathbf{k}_s = \mathbf{G}^{\mathrm{T}}\mathbf{H}^{-1}\mathbf{G}, \tag{22a, b}$$

where $\mathbf{k}_s$ is the element stiffness resulting from the nth singular hybrid element.

4.2. *Formulation of the regular element*

For the remaining region surrounding the hybrid element, we use the regular elements based upon the displacement finite element method. In the absence of body force and tractions, the total potential energy Π_{mp} to be minimized in the problem is given by

$$\Pi_{mp} = \frac{1}{2}\int_{A_m} \boldsymbol{\varepsilon}^{\mathrm{T}}\mathbf{C}\boldsymbol{\varepsilon}\, \mathrm{d}A, \tag{23}$$

where $\mathbf{C}$ is the 6×6 stiffness matrix. We now take the standard iso-parametric representation for the displacement components

$$\mathbf{u} = \mathbf{N}\mathbf{q}, \quad \boldsymbol{\varepsilon} = \mathbf{B}\mathbf{q}, \tag{24}$$

where $\mathbf{q}$ is the nodal displacement, and $\mathbf{N}$ and $\mathbf{B}$ are the shape function and the strain matrix, respectively. Substituting this equation into eqn (23), we obtain Π_{mp} in terms of the element stiffness $\mathbf{k}_r$

$$\Pi_{mp} = \tfrac{1}{2}\mathbf{q}^{\mathrm{T}}\mathbf{k}_r\mathbf{q}, \quad \mathbf{k}_r = \int_{A_m} \mathbf{B}^{\mathrm{T}}\mathbf{C}\mathbf{B}\, \mathrm{d}A, \tag{25a, b}$$

where the subscript "r" indicates the regular elements.

4.3. *Solution procedure*

The summation of the two types of element stiffness (22b) and (25b) all over the elements will yield the global stiffness $\mathbf{K}$, and the global load vector $\mathbf{Q}$ may be assembled similarly. Symbolically we may express this assemblage process as

$$\mathbf{K} = \sum_L \mathbf{k}_s + \sum_M \mathbf{k}_r, \quad \mathbf{Q} = \sum_L \mathbf{Q}_s + \sum_M \mathbf{Q}_r, \tag{26}$$

where L and M indicate the singular element number and regular element number, respectively. The discretized equilibrium equations may be written in the matrix form:

$$\mathbf{K}\mathbf{q} = \mathbf{Q}. \tag{27}$$

Imposing the displacement boundary conditions among the far field conditions, we can solve eqn (27) for the unknown nodal displacements and the reaction force. However as discussed earlier, the crack faces may be in partial contact with each other depending upon the geometry and loading, and the contact area is not known *a priori* in this case. To treat such a contact problem, which is inherently nonlinear in its nature, we should re-examine finite element analysis as the following quadratic problem:

$$\begin{aligned} &\text{Minimize} \quad \tfrac{1}{2}\mathbf{q}^{\mathrm{T}}\mathbf{K}\mathbf{q} - \mathbf{Q}^{\mathrm{T}}\mathbf{q}, \\ &\text{subject to} \quad \mathbf{A}\mathbf{q} \leqslant \mathbf{0}. \end{aligned} \tag{28}$$

Here at a contact point of crack faces the impenetrability condition is given by the inequality constraint $\mathbf{A}\mathbf{q} \leqslant \mathbf{0}$ where the $\mathbf{A}\mathbf{q}$ represents a difference of a nodal displacement at presumable contact points and the column vector $\mathbf{0}$ is a zero vector. Thus the matrix $\mathbf{A}$ is $m \times n$-dimensional where m is the number of contact pairs and n is the number of degrees of

freedom. Associated with the above problem is another problem, referred to as the Lagrangian dual problem being to maximize $\theta(\boldsymbol{\lambda})$ over $\boldsymbol{\lambda} \geqslant \mathbf{0}$, where

$$\theta(\boldsymbol{\lambda}) = \min_{\mathbf{q}} \{\tfrac{1}{2}\mathbf{q}^{\mathrm{T}}\mathbf{K}\mathbf{q} - \mathbf{Q}^{\mathrm{T}}\mathbf{q} + \boldsymbol{\lambda}^{\mathrm{T}}\mathbf{A}\mathbf{q}\}. \tag{29}$$

Note that for a given $\boldsymbol{\lambda}$, the function $\theta(\boldsymbol{\lambda})$ is strictly convex and achieves its minimum at a point satisfying

$$\mathbf{K}\mathbf{q} - \mathbf{Q} + \mathbf{A}^{\mathrm{T}}\boldsymbol{\lambda} = \mathbf{0}. \tag{30}$$

When an appropriate boundary condition is imposed, $\mathbf{K}$ is reduced to a positive definite matrix $\hat{\mathbf{K}}$, so that $\hat{\mathbf{K}}^{-1}$ exists, and then the unique solution to eqn (30) is given by

$$\hat{\mathbf{q}} = \hat{\mathbf{K}}^{-1}(\hat{\mathbf{Q}} - \hat{\mathbf{A}}^{\mathrm{T}}\boldsymbol{\lambda}), \tag{31}$$

where the superscript "$\hat{}$" indicates the only active degrees of freedom. From eqns (29) and (31), it follows that

$$\theta(\boldsymbol{\lambda}) = -\tfrac{1}{2}\boldsymbol{\lambda}^{\mathrm{T}}\mathbf{D}\boldsymbol{\lambda} - \mathbf{F}^{\mathrm{T}}\boldsymbol{\lambda},$$

where $\mathbf{D}(= \hat{\mathbf{A}}\hat{\mathbf{K}}^{-1}\hat{\mathbf{A}}^{\mathrm{T}})$ has its dimensions of $m \times m$ and $\mathbf{F}(= -\hat{\mathbf{A}}\hat{\mathbf{K}}^{-1}\hat{\mathbf{Q}})$ of $m \times 1$. Rewriting the dual problem as

$$\begin{aligned} &\text{Minimize} \quad \theta(\boldsymbol{\lambda}) = \tfrac{1}{2}\boldsymbol{\lambda}^{\mathrm{T}}\mathbf{D}\boldsymbol{\lambda} + \mathbf{F}^{\mathrm{T}}\boldsymbol{\lambda}, \\ &\text{subject to} \quad \boldsymbol{\lambda} \geqslant \mathbf{0}, \end{aligned}$$

we obtain the standard quadratic problem. Then using Lemke's algorithm (Lemke, 1968), wherein the converged solution is attained through a finite number of iterations, we can solve the above standard quadratic problem efficiently. Once $\boldsymbol{\lambda}$ is obtained through this algorithm, then the nodal displacements $\mathbf{q}$ are determined from eqn (31) and the free constant $\boldsymbol{\beta}$ is the asymptotic representation can be from eqn (21), which will complete the solution.

It is noted that displacement solution is for the composite domain consisting of the singular hybrid element and the displacement based regular elements. The theoretical basis for using two such different variational principles has been treated in Gurtin (1980).

5. NUMERICAL RESULTS AND DISCUSSION

In this section, using the field solution, obtained from the foregoing development, we compute the fracture mechanics parameters such as stress intensity factor and energy release rate. On the basis of this result, we then discuss the fracture behavior of the delamination cracks.

The following material data (graphite epoxy T300/5208) are used for numerical computation:

$$\begin{aligned} E_{\mathrm{L}} &= 134\ \mathrm{GPa}, & E_{\mathrm{T}} &= E_{\mathrm{Z}} = 10.2\ \mathrm{GPa}, \\ G_{\mathrm{LT}} &= G_{\mathrm{LZ}} = 5.52\ \mathrm{GPa}, & G_{\mathrm{TZ}} &= 3.43\ \mathrm{GPa}, \\ \nu_{\mathrm{LT}} &= \nu_{\mathrm{LZ}} = 0.3, & \nu_{\mathrm{TZ}} &= 0.49, \end{aligned}$$

where the subscripts L, T and Z indicate the longitudinal, transverse and thickness direction, respectively.

In constructing the singular hybrid finite element it is sufficient to consider only the upper right part of the unit cell for the plane strain extension and the antiplane shear

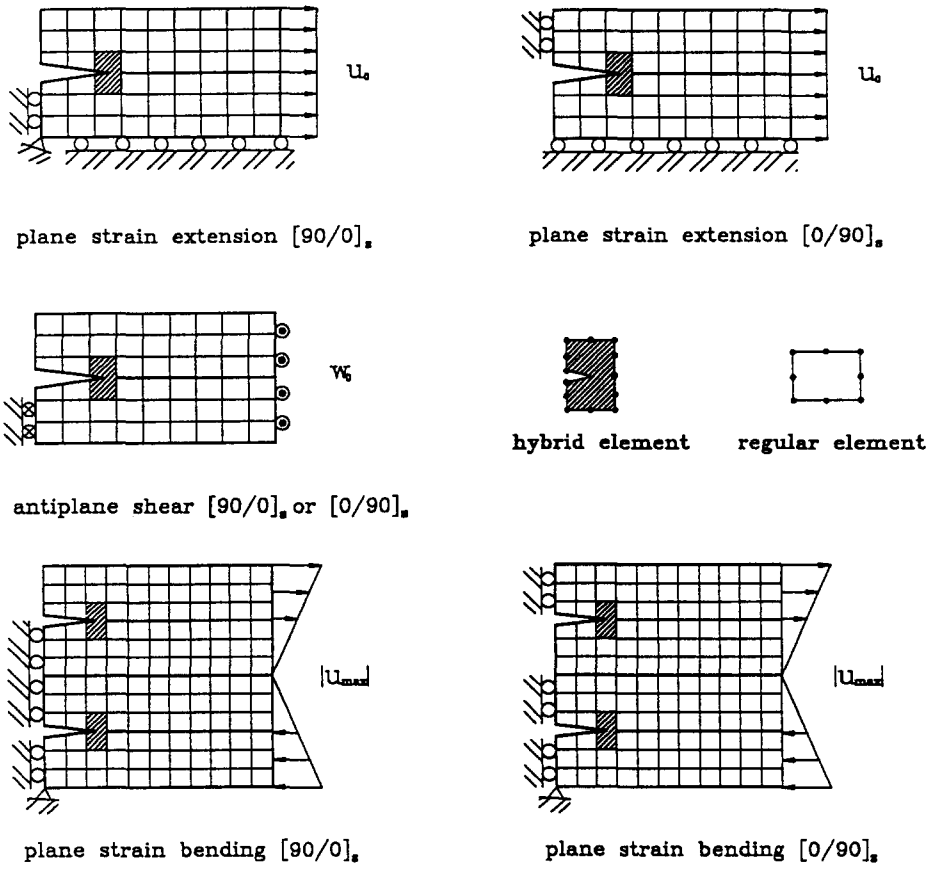

Fig. 2. Mesh configurations for singular hybrid finite element method.

because of symmetry in loading and geometry; on the other hand only the right half of the unit cell is considered for the case of plane strain bending (see Fig. 2).

The nominal strains of plane strain extension and antiplane shear are respectively defined as $\varepsilon_0 = u_0/b$ and $\gamma_0 = w_0/b$ where u_0 and w_0 are displacements imposed at $x_1 = b-c$ when $x_1 = -c$ is fixed (b is a half of the unit cell width and c is a half of the crack length). The linearly distributed nominal strain with the maximum absolute value $|\varepsilon_{\max}| = |u_{\max}|/b$ for the plane strain bending is imposed at $x_1 = b-c$ when $x_1 = -c$ is fixed. For the plane strain bending, there is no geometrical symmetry of cross-section about the mid-plane in case the crack faces contact each other, and therefore the neutral plane will not coincide with the mid-plane. To obtain a pure bending, we employ the Newton method through numerical differentiation of the equation resulting from the conditions of the net zero axial force.

The eigenvalues of each deformation obtained from the characteristic equations (see Section 3) are given as

$n-\frac{1}{2}\pm i\eta$ and n for the opened cracks under plane strain deformation,

$n-\frac{1}{2}$ and n for the closed cracks under plane strain deformation,

$n-\frac{1}{2}$ and n for the cracks under antiplane shear deformation,

($n = 0, 1, 2, 3, \ldots$ and $\eta = 0.0329\ldots$).

One of the two eigensolutions either for open or closed cracks needs to be chosen in the case of the plane strain deformation for constructing the hybrid crack tip element. In general, however, we do not know *a priori* whether the crack tip is open or closed. Then

we first perform the regular finite element analysis to find out the crack-tip behavior, and based upon this regular FEM result we choose one of the two asymptotic solutions. For all cases of loading we consider here, the crack tip is found to be opened, and the stress singularity is oscillatory for the plane strain problems.

The stress intensity factor is a fracture parameter characterizing the near-tip stress field. However, for interface cracks in anisotropic solids there has been an ambiguity in the definition of the stress intensity factors related to normalization of the eigenvector, and such vagueness was clarified by Suo (1990), who showed that due to anisotropy the form of complex stress intensity factor does not come to the same form as the complex stress intensity factor defined in interfacial cracks of isotropic bi-material, but it depends upon the way the eigenvector is normalized. Thus the definite descriptions of stress intensity factor must precede in order to use it as a fracture parameter in anisotropic composite laminates. Following Suo (1990), we define the stress intensity factor **K** for the plane strain deformation modes as (see Appendix B for detail)

$$\left(\frac{H_{22}}{H_{11}}\right)^{1/2}\sigma_{22}(r,0)+\mathrm{i}\sigma_{12}(r,0)=\frac{\mathbf{K}r^{\mathrm{i}\eta}}{\sqrt{2\pi r}},$$

as r approaches zero ahead of the crack tip, where H_{11} and H_{22} are given by eqn (B7) in Appendix B. The mode III of antiplane deformation is decoupled from plane strain deformation in orthotropic materials such as cross-ply laminates, and the stress singularity for such antiplane deformation is not oscillatory as discussed above, and the stress intensity factor is well defined as the classical mode III intensity factor:

$$\sigma_{23}(r,0)=\frac{K_{\mathrm{III}}}{\sqrt{2\pi r}}\quad \text{as } r\to 0.$$

As pointed out by Suo (1990), three real scalars (one complex stress intensity factor **K** and one real stress intensity factor K_{III}) characterize the near-tip field of an interfacial crack. However, the complex intensity factor **K** has the length scale dependency, and we therefore use the following stress intensity factor based upon the traction on a specific reference length $\hat{r}$ (Rice, 1988)

$$\frac{\mathbf{K}r^{\mathrm{i}\eta}}{\sqrt{2\pi r}}=\frac{\mathbf{K}\hat{r}^{\mathrm{i}\eta}}{\sqrt{2\pi r}}\left(\frac{r}{\hat{r}}\right)^{\mathrm{i}\eta}=\frac{(K_1+\mathrm{i}K_2)}{\sqrt{2\pi r}}\left(\frac{r}{\hat{r}}\right)^{\mathrm{i}\eta},$$

where $\hat{r}$ is chosen to be $\hat{r}/b=0.005$ (or $\hat{r}/c_0=0.02$, c_0: initial crack length).

To confirm the singular hybrid finite element solution, in Table 1 we check the solution convergence versus the number of eigenvalues in terms of the stress intensity factor based upon the above definition. We also compare the present solution with the results reported by Kim *et al.* (1991), who employed the boundary collocation method to treat the plane strain extension. The solutions from these two different methods show an excellent agreement for not too small crack lengths for the $[90/0]_s$ laminates (see the case of $[90/0]_s$ in Fig. 3). As the crack length becomes short compared with the ligament length of the crack, however, the boundary collocation method fails to yield an accurate solution. This fact is numerically confirmed by non-negligible boundary residuals along the remote boundary conditions in the resulting solution regardless of the number of eigenvalues retained (see Table 2). Moreover, as opposed to the result from Kim *et al.* (1991), the crack faces of the $[0/90]_s$ laminates under plane strain extension are not fully closed; the greater part of the crack faces are found to be closed, but a small region near the crack tip is to be opened.

Figure 3 shows the energy release rate versus the crack length for the plane strain extension (see Appendix B for calculation of energy release rate). The results from Kim *et al.* (1991), which was obtained from the boundary collocation method (BCM) are also shown for comparison. For the $[90/0]_s$ laminates, the results from the BCM are in good

Table 1. Solution convergence versus the number of eigenvalues in terms of the stress intensity factors

No. of eigenvalues	Plane strain extension				Plane strain bending (tension side)				Antiplane shear
	$[90/0]_s$ (53 elements)		$[0/90]_s$ (203 elements)		$[90/0]_s$ (212 elements)		$[0/90]_s$ (212 elements)		$[90/0]_s$ and $[0/90]_s$ (53 elements)
	K_1/ε_0	K_2/ε_0	K_1/ε_0	K_2/ε_0	$K_1/\lvert\varepsilon_{max}\rvert$	$K_2/\lvert\varepsilon_{max}\rvert$	$K_1/\lvert\varepsilon_{max}\rvert$	$K_2/\lvert\varepsilon_{max}\rvert$	K_{III}/γ_0
7	3.3128	3.1980	0.0615	−4.6206	2.9008	1.9898	0.1254	−1.1270	2.6648
11	3.3036	3.1917	0.0902	−4.6309	2.8854	1.9581	0.1346	−1.1262	2.6640
15	3.2594	3.1824	0.1172	−4.6144	2.8658	1.9507	0.1181	−1.1176	2.6643
19	3.2639	3.1862	0.1130	−4.6154	2.8668	1.9527	0.1205	−1.1176	2.6640

$\varepsilon_0 = \gamma_0 = 1$, $|\varepsilon_{max}| = 1/2$, $h_{90}/h_0 = 1$, $h_{90}/b = 1/4$, $c/b = 1/4$.
Unit: GPa $m^{-1/2}$.

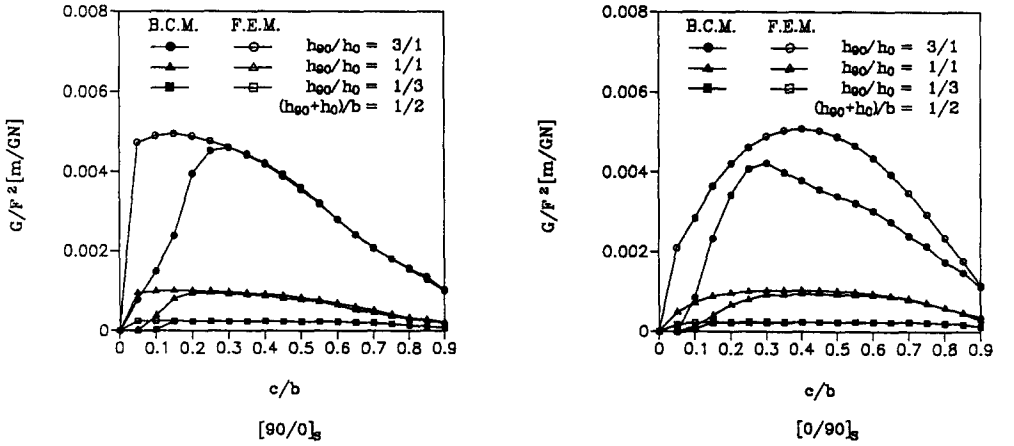

Fig. 3. Energy release rate vs the length of delamination crack under a fixed loading condition in plane strain extension [BCM indicates the results from the boundary collocation method, reported by Kim *et al.* (1991)].

agreement with the present results from the singular hybrid FEM for cracks of not too small crack length. When the crack length becomes smaller, as discussed earlier, the asymptotic solution fails to represent the far-field solution and the remote boundary residuals become significantly large in BCM. This explains the discrepancy for small crack length. For the $[0/90]_s$ laminates, there exists a significant discrepancy between the two solutions. This is due to the fact that a small open region near the crack tip was neglected and that the entire crack faces were assumed to be fully closed for the $[0/90]_s$ in Kim *et al.* (1991). Figures 4 and 5 show the results for the antiplane shear and the plane strain bending.

It is worthwhile to note that the energy release rate tends to infinity for vanishing crack length under antiplane shear while the limiting values of the energy release rate for the vanishing crack length tend to zero under plane strain extension and bending. These phenomena can be predicted from the following: the 90° ply laminate is stiffer than the 0° ply laminate under the present antiplane shear loading, and transverse cracks perpendicularly terminating at the interface have singularity stronger than the inverse square root under this loading; under plane strain extension or bending, on the other hand, the 90° ply

Table 2. Maximum boundary residuals versus crack lengths in boundary collocation method

Crack length (c/b)	No. of eigenvalues (120 collocations)	K_1/ε_0	K_2/ε_0	|Max. mismatch| along homogeneous boundary when the boundary data are 0(1)
	83	3.1993	3.1230	0.0214
0.25	63	3.1951	3.1239	0.0376
	43	2.8666	2.9416	0.0970
	83	3.2667	3.1331	0.0945
0.20	63	3.2646	3.1176	0.1101
	43	2.9934	2.8989	0.1811
	83	3.0250	2.8094	0.1775
0.15	63	3.0594	2.8013	0.1744
	43	2.9439	2.7339	0.1689
	83	2.2900	2.3907	0.3866
0.10	63	2.3977	1.2762	0.3533
	43	1.9535	1.1649	0.3809
	83	1.8823	−0.2283	0.4770
0.05	63	1.9018	−0.2008	0.4730
	43	1.4559	−0.2098	0.5141

$[90/0]_s$ plane strain extension.
Unit: GPa $m^{-1/2}$.
$\varepsilon_0 = 1$, $h_{90}/h_0 = 1$, $h_{90}/b = 1/4$.

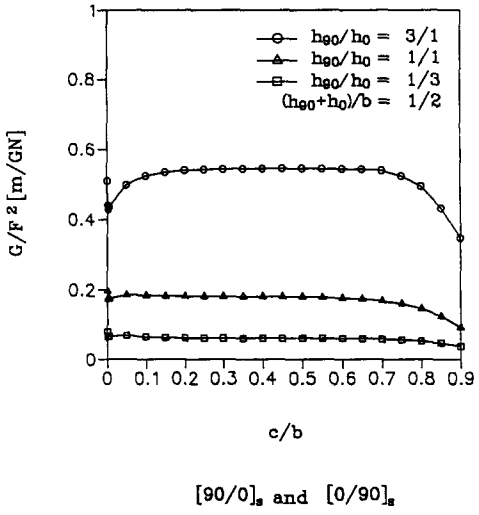

Fig. 4. Energy release rate vs the length of delamination crack under a fixed loading condition in antiplane shear.

laminate is softer than the 0° ply laminate and the transverse cracks have singularities weaker than the inverse square root (Im and Kim, 1989). Thus, the energy release rate for a vanishing delamination crack in each case tends to infinity and zero, respectively. Figures 3–5 also clearly show the effects of ply thickness ratio. That is, as the 90° ply thickness increases compared with the 0° ply thickness, the energy release rate shows a very sharp increase, which reveals the more unstable crack growth behavior. This is consistent with the observation that the energy release rate will ultimately remain constant regardless of the crack length, just as in the case of thin films, when the thickness of the 90° ply becomes smaller and smaller.

As is seen from Fig. 5, the energy release rate for the crack on the compression side under the plane strain bending is negligibly small compared with the energy release rate on the tension side. This means that only the delamination crack on the tension side will grow as the load increases. The energy release rate for the plane strain bending with cracks only on the tension side is denoted in Fig. 6 by the darkened mark, which does not show a significant difference from the case of cracks on both of the tension and compression sides.

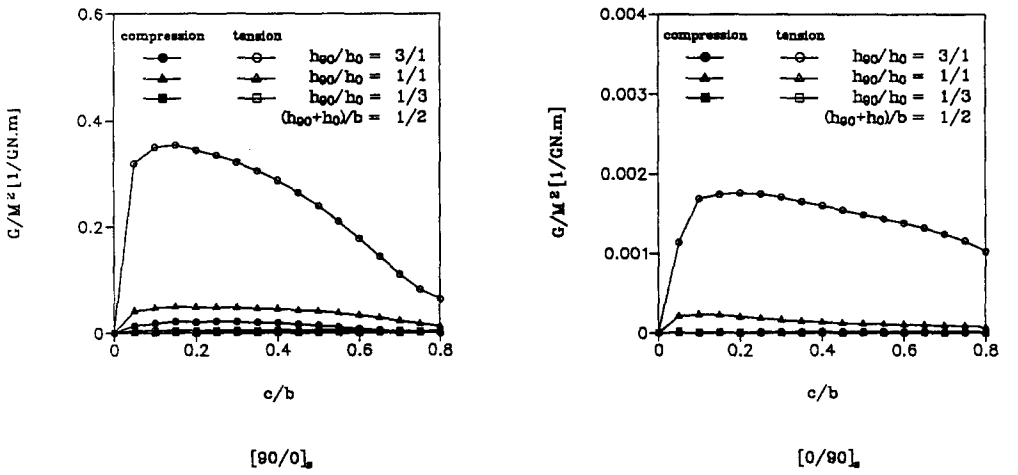

Fig. 5. Energy release rate vs the length of delamination crack under a fixed loading condition in plane strain bending.

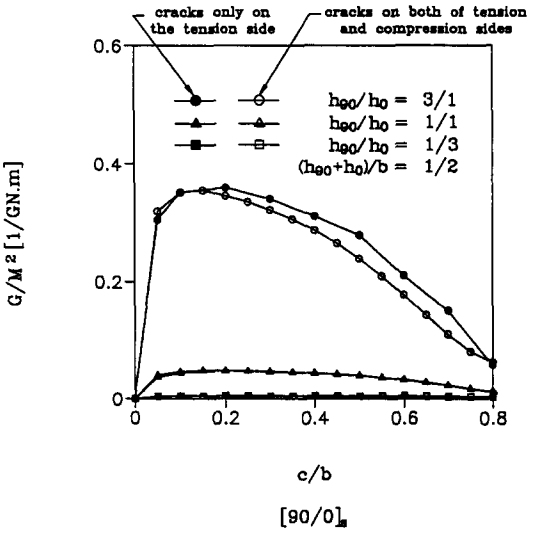

Fig. 6. Comparison of two crack configurations: One is for the case with cracks only on the tension side and the other is for the case with cracks on both the tension and compression sides.

For brittle orthotropic materials under plane strain deformation, the complex stress intensity factor **K** fully characterizes the near-tip stress field for an interfacial delamination crack, and the crack will grow when this complex scalar **K** or a set of two real stress intensity factors K_1 and K_2 in $\mathbf{K}\hat{r}^{i\eta} = K_1 + iK_2$ reaches some critical values. A combination of two real numbers K_1 and K_2 for which the crack growth begins will form a failure curve in the K_1–K_2 surface. In terms of the energy release rate, the energy release rate itself is not enough to characterize the crack tip stress field, but the phase angle is needed for another variable

$$\hat{\Psi} = \tan^{-1}\left|\frac{K_2}{K_1}\right|.$$

Now the two real parameters G and $\hat{\Psi}$ can replace the two scalars K_1 and K_2, and the crack growth criterion may be stated as

$$G = G_c(\hat{\Psi}),$$

where G_c is the critical energy release rate, which is a material constant depending upon the

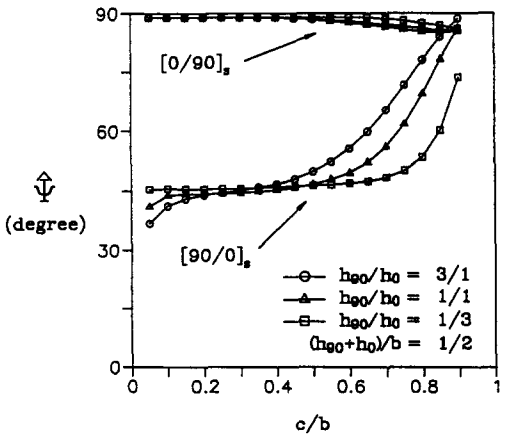

Fig. 7. Phase angle vs the length of delamination crack in plane strain extension.

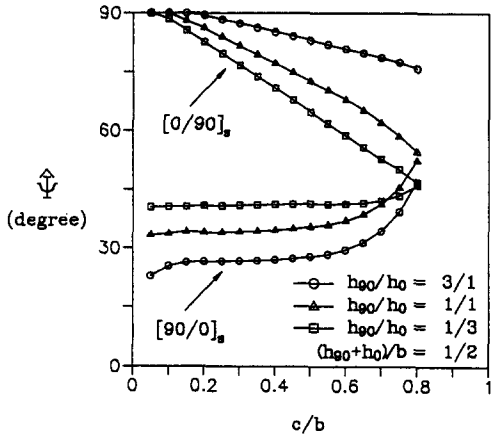

Fig. 8. phase angle vs the length of delamination crack in plane strain bending.

phase angle. Figures 7 and 8 show the phase angle defined at $\hat{r}/b = 0.005$ depending upon the crack length and the ply thickness ratios for plane strain deformation. It is noticed that the phase angle is close to $\pi/2$ for $[0/90]_s$ regardless of the crack length under plane strain extension, so that mode II is dominant over mode I. In $[90/0]_s$ laminates the phase angle remains relatively uniform for the crack length of $c/b = 0 \sim 0.5$ for both plane strain extension and bending (Figs 7 and 8), while for $[0/90]_s$ laminates the phase angle is almost constant for plane strain extension (Fig. 7), and it gradually decreases for plane strain bending (Fig. 8). In general, the resistance to crack growth is an increasing function of $\hat{\Psi}$ (G_c for mode II is greater than G_c for mode I). Since $\hat{\Psi}$ is uniform or gradually decreases for $c/b = 0 \sim 0.5$, and the crack length corresponding to the maximum G is within this range in Figs 3 and 5, there will exist an inherently built-in crack arrest mechanism: Any delamination crack will undergo unstable growth until the crack length reaches a critical value associated with the maximum G, and it will continue to grow under a fixed loading until the energy release rate decreases to the critical value $G_c(\hat{\Psi})$. For the antiplane shear, the crack growth criterion is given by $G = G_c$, where the critical energy release rate G_c for mode III is a material constant. As is seen in Fig. 4, the energy release rate G versus the crack length curve for the antiplane shear is relatively flat except for large values of G for vanishing crack length.

Acknowledgements—This study has been supported by the Korea Science and Engineering Foundation (KOSEF) under Grant No. 89-04-05-02. The authors gratefully acknowledge the grant to KAIST from KOSEF.

REFERENCES

Atluri, S. N. and Nakagaki, M. (1986). Computational methods for plane problems of fracture. In *Computational Methods in Mechanics of Fracture* (Edited by S. N. Atluri), pp. 169–227. Elsevier, Amsterdam.

Bogy, D. B. (1971). On the plane elastostatic problem of a load crack terminating at a material interface. *J. Appl. Mech.* **38,** 911–918.

Dempsey, J. P. and Sinclair, G. B. (1979). On the stress singularities in plane elasticity of the composite wedge. *J. Elasticity* **9,** 373–391.

Gurtin, M. E. (1980). On patched variational principles in elasticity. *J. Elasticity* **10,** 329–332.

Im, S. (1989). Asymptotic stress field around a crack normal to the ply-interface of an anisotropic composite laminate. *Int. J. Solids Structures* **26,** 111–127.

Im, S. and Kim, T. W. (1989). Stress field near transverse cracks under extension or in-plane shear in cross-ply composite laminates. *KSME Jl* **3,** 121–129.

Kim, T. W., Kim, H. J. and Im, S. (1991). Delamination crack originating from transverse cracking in cross-ply composite laminates under extension. *Int. J. Solids Structures* **27,** 1925–1941.

Lemke, C. E. (1968). On complementary pivot theory. In *Mathematics of the Decision Sciences* (Edited by G. B. Dantzig and A. F. Veinott), pp. 95–114. American Mathematical Society, New York.

Lim, S. K. (1988). Transverse failure in cross-ply laminated composites. Ph.D. Thesis, Korea Advanced Institute of Science and Technology.

Pipes, R. B. and Pagano, N. J. (1970). Interlaminar stresses in composite laminates under uniform axial extension. *J. Comp. Mater.* **4,** 538–548.

Rice, J. R. (1988). Elastic fracture mechanics concepts for interface cracks. *J. Appl. Mech.* **55,** 98–103.

Stolarski, H. K. and Chiang, M. Y. M. (1989). On the significance of the logarithmic term in the free edge stress singularity of composite laminates. *Int. J. Solids Structures* **25,** 75–93.
Suo, Z. (1990). Singularities, interfaces and cracks in dissimilar anisotropic media. *Proc. R. Soc. Lond. A* **427,** 331–358.
Ting, T. C. T. (1986). Explicit solution and invariance of the singularities at an interface crack in anisotropic composites. *Int. J. Solids Structures* **22,** 965–983.
Ting, T. C. T. and Chou, S. C. (1981). Edge singularities in anisotropic composites. *Int. J. Solids Structures* **17,** 1057–1068.
Ting, T. C. T. and Hoang, P. H. (1984). Singularities at the tip of a crack normal to the interface of an anisotropic layered composite. *Int. J. Solids Structures* **20,** 430–454.
Wang, S. S. (1984). Edge delamination in angle-ply composite laminates. *AIAA Jl* **22,** 256–264.
Wang, S. S. and Choi, I. (1982). Boundary-layer effect in composite laminates. Part I—free-edge stress singularities; Part II—free-edge stress solutions and characteristics. *J. Appl. Mech.* **49,** 541–550.
Wang, S. S. and Choi, I. (1983). The mechanics of delamination in fiber composite materials. Part I—stress singularities. NASA-CR-172269, National Aeronautics and Space Administration, Langley Research Center, Hampton, VA.
Wang, S. S. and Yuan, F. G. (1983). A hybrid finite element approach to composite laminate elasticity problems with singularities. *J. Appl. Mech.* **50,** 835–844.
Washizu, K. (1988). *Variational, Methods in Elasticity and Plasticity* (3rd Edn). Pergamon Press, Oxford.
Williams, M. L. (1959). The stress around a fault or crack in dissimilar media. *Bull. Seismol. Soc. Am.* **49,** 199–204.
Zwiers, R. I., Ting, T. C. T. and Spilker, R. L. (1982). On the logarithmic singularity of free-edge stress in laminated composites under uniform extension. *J. Appl. Mech.* **49,** 562–569.

APPENDIX A

For antiplane shear, we have the following expression for $Q_{n3}^{(m)}$ and $P_{n3\alpha}^{(m)}$ of eqn (13a, b),

$$u_3^{(m)} = \sum_{n=1}^{\infty} Q_{n3}^{(m)}, \quad \sigma_{3\alpha}^{(m)} = \sum_{n=1}^{\infty} P_{n3\alpha}^{(m)}, \tag{A1a, b}$$

$$Q_{n3}^{(m)} = \gamma_{1n}\,\mathrm{Re}\,[\psi_{n3}^{(m)}] + \gamma_{2n}\,\mathrm{Im}\,[\psi_{n3}^{(m)}],$$
$$P_{n3\alpha}^{(m)} = \gamma_{1n}\,\mathrm{Re}\,[\phi_{n3\alpha}^{(m)}] + \gamma_{2n}\,\mathrm{Im}\,[\phi_{n3\alpha}^{(m)}],$$
$$\psi_{n3}^{(m)} = (a_{1n}^{(m)} v_{31}^{(m)} s_1^{(m)\delta_n+1} + a_{2n}^{(m)} \bar{v}_{31}^{(m)} \bar{s}_1^{(m)\delta_n+1})/(\delta_n+1),$$
$$\phi_{n3\alpha}^{(m)} = a_{1n}^{(m)}(C_{3\alpha31}^{(m)} + \xi_1^{(m)} C_{3\alpha32}^{(m)}) v_{31}^{(m)} s_1^{(m)\delta_n} + a_{2n}^{(m)}(C_{3\alpha31}^{(m)} + \bar{\xi}_1^{(m)} C_{3\alpha32}^{(m)}) \bar{v}_{31}^{(m)} \bar{s}_1^{(m)\delta_n}$$

for complex δ_n, $\mathrm{Im}\,[\delta_n] > 0$, or

$$Q_{n3}^{(m)} = \gamma_{3n}\,\mathrm{Re}\,[a_{1n}^{(m)} v_{31}^{(m)} s_1^{(m)\delta_n+1}/(\delta_n+1)],$$
$$P_{n3\alpha}^{(m)} = \gamma_{3n}\,\mathrm{Re}\,[a_{1n}^{(m)}(C_{3\alpha31}^{(m)} + \xi_1^{(m)} C_{3\alpha32}^{(m)}) v_{31}^{(m)} s_1^{(m)\delta_n}]$$

for real δ_n.

For plane strain deformation, $Q_{n\alpha}^{(m)}$ and $P_{n\alpha\beta}^{(m)}$ of eqn (14a, b) are given as

$$u_\alpha^{(m)} = \sum_{n=1}^{\infty} Q_{n\alpha}^{(m)}, \quad \sigma_{\alpha\beta}^{(m)} = \sum_{n=1}^{\infty} P_{n\alpha\beta}^{(m)}, \tag{A2a, b}$$

$$Q_{n\alpha}^{(m)} = \gamma_{1n}\,\mathrm{Re}\,[\psi_{n\alpha}^{(m)}] + \gamma_{2n}\,\mathrm{Im}\,\psi_{n\alpha}^{(m)}],$$
$$P_{n\alpha\beta}^{(m)} = \gamma_{1n}\,\mathrm{Re}\,[\phi_{n\alpha\beta}^{(m)}] + \gamma_{2n}\,\mathrm{Im}\,[\phi_{n\alpha\beta}^{(m)}],$$
$$\psi_{n\alpha}^{(m)} = \sum_{k=1}^{2} \{(b_{kn}^{(m)} v_{\alpha k}^{(m)} z_k^{(m)\delta_n+1} + b_{(k+2)n}^{(m)} \bar{v}_{\alpha k}^{(m)} \bar{z}_k^{(m)\delta_n+1})/(\delta_n+1)\},$$
$$\phi_{n\alpha\beta}^{(m)} = \sum_{k=1}^{2}\sum_{\gamma=1}^{2} \{b_{kn}^{(m)}(C_{\alpha\beta\gamma1}^{(m)} + \mu_k^{(m)} C_{\alpha\beta\gamma2}^{(m)}) v_{\gamma k}^{(m)} z_k^{(m)\delta_n} + b_{(k+2)n}^{(m)}(C_{\alpha\beta\gamma1}^{(m)} + \bar{\mu}_k^{(m)} C_{\alpha\beta\gamma2}^{(m)}) \bar{v}_{\gamma k}^{(m)} \bar{z}_k^{(m)\delta_n}\}$$

for complex δ_n, $\mathrm{Im}\,[\delta_n] > 0$, or

$$Q_{n\alpha}^{(m)} = \gamma_{3n}\,\mathrm{Re}\left[\sum_{k=1}^{2} b_{kn}^{(m)} v_{\alpha k}^{(m)} z_k^{(m)\delta_n+1}/(\delta_n+1)\right],$$
$$P_{n\alpha\beta}^{(m)} = \gamma_{3n}\,\mathrm{Re}\left[\sum_{k=1}^{2}\sum_{\gamma=1}^{2} b_{kn}^{(m)}(C_{\alpha\beta\gamma1}^{(m)} + \mu_k^{(m)} C_{\alpha\beta\gamma2}^{(m)}) v_{\gamma k}^{(m)} z_k^{(m)\delta_n}\right]$$

for real δ_n,

where the normalized eigenvectors $a_{\alpha n}^{(m)}$ are given in eqn (12b), and $b_{kn}^{(m)}$ are given in a similar fashion.

APPENDIX B

In this Appendix, based upon the asymptotic representation at the near-tip field Suo's stress intensity factor (Suo, 1990) and the energy release rate for interfacial cracks are derived in orthotropic materials.

We take the first term of the asymptotic solution $\sigma_{2\alpha}$ ($\alpha = 1, 2$) along the ply interface ($x_1 \geqslant 0$), described in Appendix A, and rewrite it as

$$\sigma_{21}|_{\delta_1 = -1/2+i\eta} = \gamma_{11}\,\mathrm{Re}\,[2w_1 r^{i\eta}]r^{-1/2} + \gamma_{21}\,\mathrm{Im}\,[2w_1 r^{i\eta}]r^{-1/2}$$
$$= 2(2\pi r)^{-1/2}\,\mathrm{Re}\,[\sqrt{2\pi}(\gamma_{11} - i\gamma_{21})r^{i\eta}w_1], \tag{B1a}$$

$$\sigma_{22}|_{\delta_1 = -1/2+i\eta} = \gamma_{11}\,\mathrm{Re}\,[2w_2 r^{i\eta}]r^{-1/2} + \gamma_{21}\,\mathrm{Im}\,[2w_2 r^{i\eta}]r^{-1/2}$$
$$= 2(2\pi r)^{-1/2}\,\mathrm{Re}\,[\sqrt{2\pi}(\gamma_{11} - i\gamma_{21})r^{i\eta}w_2], \tag{B1b}$$

where the eigenvectors w_1 and w_2 are

$$2w_1 = \sum_{k=1}^{2}\sum_{\gamma=1}^{2}\{b_{k1}(C_{21\gamma 1} + \mu_k C_{21\gamma 2})v_{\gamma k} + b_{(k+2)1}(C_{21\gamma 1} + \bar{\mu}_k C_{21\gamma 2})\bar{v}_{\gamma k}\}, \tag{B2a}$$

$$2w_2 = \sum_{k=1}^{2}\sum_{\gamma=1}^{2}\{b_{k1}(C_{22\gamma 1} + \mu_k C_{22\gamma 2})v_{\gamma k} + b_{(k+2)1}(C_{22\gamma 1} + \bar{\mu}_k C_{22\gamma 2})\bar{v}_{\gamma k}\}. \tag{B2b}$$

Setting $\mathbf{K} = \sqrt{2\pi}(\gamma_{11} - i\gamma_{21})$, eqn (B1a, b) can be written as

$$\sigma_{21}(r, 0) = 2(2\pi r)^{-1/2}\,\mathrm{Re}\,[\mathbf{K}r^{i\eta}w_1], \tag{B3a}$$

$$\sigma_{22}(r, 0) = 2(2\pi r)^{-1/2}\,\mathrm{Re}\,[\mathbf{K}r^{i\eta}w_2]. \tag{B3b}$$

The stress intensity factor $\mathbf{K}$ becomes different in accordance with the method of normalizing the eigenvectors b_{k1} ($k = 1, 2, 3, 4$) or the resulting eigenvectors w_α ($\alpha = 1, 2$).

To obtain the relation between b_{k1} and w_α we introduce the matrix $L_{\alpha\beta}$ as

$$L_{\alpha\beta}^{(m)} = \sum_{\gamma=1}^{2}(C_{\alpha 2\gamma 1}^{(m)} + \mu_\beta^{(m)} C_{\alpha 2\gamma 2}^{(m)})v_{\gamma\beta}^{(m)} \quad (m = 1, 2),$$

and apply the traction free and continuity condition at the near-tip field to the asymptotic solution

$$b_{\alpha 1}^{(1)} = \frac{e^{\pi\eta}}{\cosh \pi\eta}\sum_{\beta=1}^{2} L_{\alpha\beta}^{(1)-1}w_\beta, \qquad b_{\alpha 1}^{(2)} = \frac{e^{-\pi\eta}}{\cosh \pi\eta}\sum_{\beta=1}^{2} L_{\alpha\beta}^{(2)-1}w_\beta,$$

$$b_{(\alpha+2)1}^{(1)} = \frac{e^{-\pi\eta}}{\cosh \pi\eta}\sum_{\beta=1}^{2} \bar{L}_{\alpha\beta}^{(1)-1}w_\beta, \quad b_{(\alpha+2)1}^{(2)} = \frac{e^{\pi\eta}}{\cosh \pi\eta}\sum_{\beta=1}^{2} \bar{L}_{\alpha\beta}^{(2)-1}w_\beta. \tag{B4}$$

To determine the eigenvectors w_1 and w_2 we apply the displacement continuity along the ply interface for the first term of asymptotic displacement solution u_α ($\alpha = 1, 2$) described in Appendix A

$$\sum_{\beta=1}^{2}(v_{\alpha\beta}^{(1)}b_{\beta 1}^{(1)} + \bar{v}_{\alpha\beta}^{(1)}b_{(\beta+2)1}^{(1)}) = \sum_{\beta=1}^{2}(v_{\alpha\beta}^{(2)}b_{\beta 1}^{(2)} + \bar{v}_{\alpha\beta}^{(2)}b_{(\beta+2)1}^{(2)}), \tag{B5}$$

and substitute eqn (B4) into eqn (B5)

$$e^{\pi\eta}\sum_{\beta=1}^{2}\sum_{\gamma=1}^{2}(v_{\alpha\beta}^{(1)}L_{\beta\gamma}^{(1)-1} - \bar{v}_{\alpha\beta}^{(2)}\bar{L}_{\beta\gamma}^{(2)-1})w_\gamma = e^{-\pi\eta}\sum_{\beta=1}^{2}\sum_{\gamma=1}^{2}(v_{\alpha\beta}^{(2)}L_{\beta\gamma}^{(2)-1} - \bar{v}_{\alpha\beta}^{(1)}\bar{L}_{\beta\gamma}^{(1)-1})w_\gamma. \tag{B6}$$

Following Suo (1990), we introduce the matrix $B_{\alpha\beta}$ and $H_{\alpha\beta}$

$$B_{\alpha\beta}^{(m)} = i\sum_{\gamma=1}^{2} v_{\alpha\gamma}^{(m)}L_{\gamma\beta}^{(m)-1} \quad (m = 1, 2), \qquad H_{\alpha\beta} = B_{\alpha\beta}^{(1)} + \bar{B}_{\alpha\beta}^{(2)}, \tag{B7}$$

and rewrite eqn (B6) as

$$\sum_{\beta=1}^{2}\bar{H}_{\alpha\beta}w_\beta = e^{2\pi\eta}\sum_{\beta=1}^{2}H_{\alpha\beta}w_\beta. \tag{B8}$$

From the eigenvalue equation (B8), we thus select $w_1 = -1/2i$, $w_2 = 1/2\sqrt{H_{11}/H_{22}}$ as proposed by Suo (1990) and then rewrite eqn (B3a, b) as

$$\left(\frac{H_{22}}{H_{11}}\right)^{1/2}\sigma_{22} + i\sigma_{12} = \frac{\mathbf{K}r^{i\eta}}{\sqrt{2\pi r}} \quad \text{ahead of the crack tip ligament.} \tag{B9}$$

Due to oscillatory singularity in the presence of which $\mathbf{K}$ has length scale dependency we introduce the concept of Rice (1988) such that in a reference length $\hat{r}$

$$\mathbf{K}\hat{r}^{i\eta} = K_1 + iK_2. \tag{B10}$$

Thus we obtain the stress intensity factors K_1 and K_2,

$$K_1 = \left(\frac{H_{22}}{H_{11}}\right)^{1/2} \sqrt{2\pi\hat{r}}\sigma_{22}(\hat{r}, 0), \quad K_2 = \sqrt{2\pi\hat{r}}\sigma_{12}(\hat{r}, 0). \tag{B11}$$

By use of asymptotic representation of displacement u_α and the relation between b_{k1} and w_α the displacement jump behind the crack tip can be written as

$$\left(\frac{H_{11}}{H_{22}}\right)^{1/2} \Delta u_2 + i\Delta u_1 = \frac{2H_{11}\mathbf{K}r^{1/2+i\eta}(2\pi)^{-1/2}}{(1+2i\eta)\cosh(\pi\eta)}, \tag{B12}$$

where $\Delta u_2 = u_2(r, \pi) - u_2(r, -\pi)$, $\Delta u_1 = u_1(r, \pi) - u_1(r, -\pi)$. Applying (B9) and (B12) to Irwin's virtual crack extension concept, the energy release rate related to the stress intensity factor can be obtained as

$$G = G_1 + G_{II} = \frac{H_{11}|\mathbf{K}|^2}{4\cosh^2(\pi\eta)}. \tag{B13}$$

For the antiplane deformation we can define the stress intensity factor and the energy release rate for mode III as

$$K_{III} = \sqrt{2\pi r}\sigma_{23}(r, 0), \tag{B14}$$

$$G_{III} = \frac{1}{4i}(v_{31}^{(1)} + v_{31}^{(2)})K_{III}^2. \tag{B15}$$